

NUCLEAR DATA AND MEASUREMENTS SERIES

ANL/NDM-25

**Determination of the Energy Scale
for Neutron Cross Section Measurements
Employing a Monoenergetic Accelerator**

by

J.W. Meadows

January 1977

**ARGONNE NATIONAL LABORATORY,
ARGONNE, ILLINOIS 60439, U.S.A.**

NUCLEAR DATA AND MEASUREMENTS SERIES

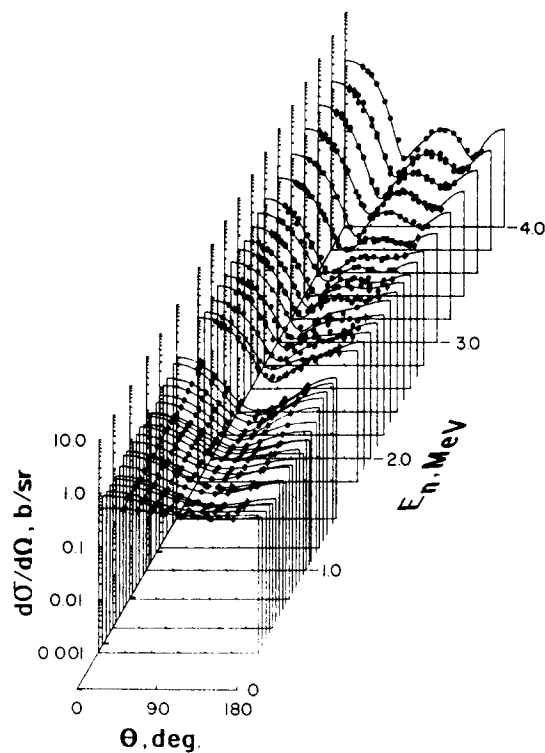
ANL/NDM-25

DETERMINATION OF THE ENERGY SCALE FOR
NEUTRON CROSS SECTION MEASUREMENTS
EMPLOYING A MONOENERGETIC ACCELERATOR

by

J. W. Meadows

January 1977



U of C. AUA. USERDA

ARGONNE NATIONAL LABORATORY,
ARGONNE, ILLINOIS 60439, U.S.A.

The facilities of Argonne National Laboratory are owned by the United States Government. Under the terms of a contract (W-31-109-Eng-38) between the U. S. Atomic Energy Commission, Argonne Universities Association and The University of Chicago, the University employs the staff and operates the Laboratory in accordance with policies and programs formulated, approved and reviewed by the Association.

MEMBERS OF ARGONNE UNIVERSITIES ASSOCIATION

The University of Arizona	Kansas State University	The Ohio State University
Carnegie-Mellon University	The University of Kansas	Ohio University
Case Western Reserve University	Loyola University	The Pennsylvania State University
The University of Chicago	Marquette University	Purdue University
University of Cincinnati	Michigan State University	Saint Louis University
Illinois Institute of Technology	The University of Michigan	Southern Illinois University
University of Illinois	University of Minnesota	The University of Texas at Austin
Indiana University	University of Missouri	Washington University
Iowa State University	Northwestern University	Wayne State University
The University of Iowa	University of Notre Dame	The University of Wisconsin

NOTICE

This report was prepared as an account of work sponsored by the United States Government. Neither the United States nor the United States Atomic Energy Commission, nor any of their employees, nor any of their contractors, subcontractors, or their employees, makes any warranty, express or implied, or assumes any legal liability or responsibility for the accuracy, completeness or usefulness of any information, apparatus, product or process disclosed, or represents that its use would not infringe privately-owned rights.

ANL/NDM-25

DETERMINATION OF THE ENERGY SCALE FOR
NEUTRON CROSS SECTION MEASUREMENTS
EMPLOYING A MONOENERGETIC ACCELERATOR

by

J. W. Meadows

January 1977

Applied Physics Division
Argonne National Laboratory
9700 South Cass Avenue
Argonne, Illinois 60439
U.S.A.

NUCLEAR DATA AND MEASUREMENTS SERIES

The Nuclear Data and Measurements Series presents results of studies in the field of microscopic nuclear data. The primary objective is the dissemination of information in the comprehensive form required for nuclear technology applications. This Series is devoted to: a) Measured microscopic nuclear parameters, b) Experimental techniques and facilities employed in data measurements, c) The analysis, correlation and interpretation of nuclear data, and d) The evaluation of nuclear data. Contributions to this Series are reviewed to assure technical competence and, unless otherwise stated, the contents can be formally referenced. This Series does not supplant formal journal publication but it does provide the more extensive information required for technological applications (e.g., tabulated numerical data) in a timely manner.

TABLE OF CONTENTS

	<u>Page</u>
ABSTRACT	3
I. INTRODUCTION	5
II. (p,n) YIELDS NEAR THRESHOLD.	6
II.A. The Yield Equation	7
II.A.1. The Reaction Cross Section	8
II.A.2. Beam Energy Distribution	9
II.A.3. Energy Loss Distribution	10
II.B. Basic Yields Curve Characteristics	11
II.C. Calculated Yield Curves.	12
II.D. Measured Yield Curves.	13
III. NEUTRON ENERGY SPECTRA FROM LITHIUM TARGETS.	14
IV. THE CARBON RESONANCE	15
V. THE TIME-OF-FLIGHT MEASUREMENT	17
VI. CONCLUSIONS.	18
REFERENCES	20
TABLES	21
FIGURES.	23

DETERMINATION OF THE ENERGY SCALE FOR
NEUTRON CROSS SECTION MEASUREMENTS
EMPLOYING A MONOENERGETIC ACCELERATOR

by

J. W. Meadows

Argonne National Laboratory, Argonne, Illinois 60439, U.S.A.

ABSTRACT

Persistent disparities between the energy scales used for broad spectrum neutron source studies and monoenergetic neutron source studies has prompted an investigation of various factors which affect the determination of an energy scale for monoenergetic accelerators. Yield curves and neutron energy spectra have been calculated for some (p,n) reactions commonly used as neutron sources or for energy calibration purposes. These calculations take into account the energy spread of the incident proton beam and the statistical nature of the proton energy loss. It is shown that when thresholds are observed by detecting the 0 deg. neutron yield the best results are obtained by plotting the square of the yield against the proton energy and extrapolating to zero yield. A linear plot can be in error by 1-2 keV if the energy spread of the proton beam is large.

* This work was performed under the auspices of the U.S. Energy Research and Development Administration.

These factors also affect the shape of the neutron energy spectrum although the average energy shows little change. A calibration was established for the Argonne Fast Neutron Generator by locating $\text{Li-7}(p,n)\text{Be-7}$ threshold (1880.60 ± 0.07 keV) and the $\text{B-11}(p,n)\text{C-11}$ threshold (3016.4 ± 1.6 keV). This calibration was confirmed and extended by measuring the location of a carbon resonance (2077 ± 2 keV neutron energy) and by a time-of-flight measurement at 4.466 MeV neutron energy. The energy scale established by this procedure was consistent within experimental error.

I. INTRODUCTION

The problem of the energy scale in U-238:U-235 fission cross section ratio measurements received considerable attention at a recent NEANDC/NEACRP Specialists Meeting on The Fission Cross Sections of U-233, U-235, U-238 and Pu-239 held June 28-30, 1976 at Argonne National Laboratory. Papers by Behrens et al., Cierjacks et al., and Evans et al. showed that the data generated by broad spectrum neutron sources are now in reasonable agreement (1). Most of these data, after renormalization, fall within a band 15-20 keV wide in the energy region below 2 MeV. However, the results from monoenergetic measurements generally lie at higher energies. Some ANL results reported at the same meeting (1) are some 20 keV above the mean of the broad spectrum measurements. The effect of this difference is small. A 20 keV energy shift changes the calculated U-238:U-235 fission cross section ratio in typical fast reactor core spectra by 1-2%. Still 20 keV is large compared to the estimated errors in the energy scales of these measurements. This state of affairs was disturbing and it suggested that additional cross checks between energy scales of the broad spectrum and monoenergetic machines were necessary. The narrow carbon resonance near 2 MeV is a common reference point for time-of-flight measurements and the recommendation was made that a measurement of the location of this resonance be made at the Argonne Fast Neutron Generator (FNG). After the completion of this measurement it became clear that additional aspects of the experimental determination of the energy calibration for monoenergetic accelerators were in need of a closer look and that

the location of the carbon resonance offered a starting point for a study of the consistency of the energy calibration of the FNG. This included scrutiny of techniques involved in locating (p,n) thresholds and the effects of the distribution of proton energy losses in lithium targets on neutron energy resolution.

This report presents the results of this investigation and, in the process, describes some procedures which can be used to improve the energy calibration for a monoenergetic accelerator.

II. (p,n) YIELDS NEAR THRESHOLD

Energy calibration by locating the thresholds of (p,n) reactions is a common practice at monoenergetic facilities including the FNG. When these accelerators are used as neutron sources the energy resolution is usually several keV or more due to the target thickness. Consequently, extremely accurate energy values (< 1 keV) are rarely required and quite casual threshold measurements are usually adequate. However, under some conditions, errors up to several keV are possible and whenever accuracies of better than 2 keV are required some problems arise.

Threshold location is a long standing problem and there is a considerable literature concerning it as well as the associated problem of locating (p, γ) resonances. References 2 thru 9 give a representative, but by no means exhaustive, survey. In the ideal approach to the problem yield curves for the reaction are calculated including such effects as beam energy spread, target conditions, fluctuations in energy loss and detector efficiency. The threshold is then adjusted to fit the calculated yield to the

experimental yield.

The above procedure is capable of very good accuracy, far better than the requirements of neutron sources, but it is complicated, time consuming and requires a knowledge of some factors that are often not too well known (e.g. beam energy spread). A more common approach is to plot some simple function of the neutron yield against proton energy and extrapolate to zero yield. Usually the total yield is measured and the threshold is located by extrapolating a plot of (yield)^{3/2} (5,9). When the accelerator is used as a neutron source the 0 deg. neutron yield is usually measured to determine the target thickness. Thus it is convenient to also determine the threshold with the same detector and it is shown in Section II.B. that a plot of (yield)² can be extrapolated linearly. In order to test this procedure, yield curves have been calculated for various experimental conditions and are compared to measured ones.

II.A. The Yield Equation

The neutron yield, Y, for a proton beam of average energy E_b striking a target thickness t is

$$Y(E_b, t) = N \int_0^t dx \int_{E_{th}}^{\infty} dE_i \int_{E_p}^{\infty} dE_p \sigma(E_p) P(E_b, E_i) W(E_p, E_i, x) \quad (1)$$

where N is the number of atoms/cm³, $\sigma(E_p)$ is the cross section for the (p,n) reaction at proton energy E_p, P(E_b, E_i) is the probability that a proton beam with average energy E_b will have a proton with energy E_i, W(E_p, E_i, x) is the probability that a proton with initial

energy E_i will have energy E_p after penetrating distance x .

II.A.I. The Reaction Cross Section

At energies just above the reaction threshold, E_{th} , the emitted particles are s-wave neutrons and, in the absence of nearby resonances, the cross section will be proportional to the center of mass neutron velocity. Thus the total (p,n) cross section has the energy dependence

$$\sigma(E_p) \propto (E_p - E_{th})^{1/2} \quad (2)$$

Equation (2) is adequate for the B-11(p,n) and the C-13(p,n) reactions but not for the Li-7(p,n) since there is a nearby resonance. Newson et al. (2) have shown that the Li-7 cross section is represented very well by 2- resonance near threshold plus a 3+ resonance at 2.25 MeV. However the 3+ resonance contributes very little near threshold so it can be assumed that only s-wave neutrons are emitted. The energy dependence of the cross section for the first 30-40 keV is given by

$$\sigma(E_p) \propto \frac{\sqrt{E_p - E_{th}}}{(1 + 4.38 \sqrt{E_p - E_{th}})^2} \quad (3)$$

Target yields are usually measured with a detector at 0 deg. and in good geometry. Since these are s-wave neutrons the differential cross section in the laboratory system is given by

$$\sigma(E_p, \theta_o) = \sigma(E_p) J(\gamma, \cos\theta) \quad (4)$$

where $J(\gamma, \cos\theta)$ is the usual transformation from the center of mass to the laboratory system and

$$\gamma = \left(\frac{m_1 m_3}{m_2 m_4} \frac{E_p}{E_p - E_{th}} \right)^{1/2} \quad (5)$$

II.A.2. Beam Energy Distribution

The energy spread of the incident beam is usually controlled by some type of spectrometer. At the FNG this spectrometer is a 90 deg. double focusing magnet with a 66 cm radius of curvature (R) and with slits located at the focal points. These points are 2R from the entrance and exit pole faces. The displacement due to energy change is

$$D = 99 \text{ dE/E cm.} \quad (6)$$

At the Li-7(p,n) threshold 1 keV is equivalent to 0.052 cm. When the pulsed and bunched beam is used the slit opening may be as wide as 0.5 cm which corresponds to 9.5 keV at the Li-7(p,n) threshold. In the extreme case energy spreads of 15-20 keV are possible since both slits are usually set to the same opening.

Of course such an extreme is never approached in practice. The beam spot has a finite size plus a considerable halo. Other restrictions in the beam transport system ensure that it passes through the center of the entrance slits parallel to the spectrometer axis and the energy control system keeps it centered in the image slits. Even with wider slit settings the energy resolution is maintained at < 2 keV. When the klystron buncher is operating an additional spread is introduced and with 0.5 cm slit settings a total energy spread of ~ 10 keV is observed. By reducing the slit openings the energy spread can be reduced to any desired value with a corresponding loss in beam current.

For the calculations in this report the energy spread was assumed to be Gaussian with the total width restricted to 4 s.

$$\begin{aligned} P(E_b, E_i) &= A \exp[-(E_b - E_i)^2 / 2s^2] \\ P(E_b, E_i) &= 0 \quad |E_b - E_i| > 2s \end{aligned} \quad (7)$$

II.A.3. Energy Loss Distribution

It is usually assumed that the energy loss by a charged particle passing through an absorber depends only on the thickness of the absorber. However energy is lost in discrete amounts through particle-electron collision and there are statistical fluctuations. For thin absorbers these fluctuations may be of the same magnitude as the average energy loss.

A general solution of this problem has been given by Symon (9). In a strict sense his results are not applicable to this situation because of some of the assumptions made to obtain numerical results (e.g. a particle velocity high compared to the electron orbital velocity and the ignoring of distant collisions) but it is available and at least one other investigator has found it to be adequate (4). Symon's results are found in an unpublished Ph.D thesis. The material used in these calculations was taken from a summary by Rossi (10).

The parameters of Symon's distribution are functions of a quantity, G , which is the ratio of an energy term that is related to the width of the distribution and of the maximum energy that can be transferred to a stationary free electron in a single collision. If numbers are put in for protons and lithium and if $v^2/c^2 \ll 1$

$$G = 14300 x/E_p^2$$

where x is the depth of penetration in grams/cm^2 and E_p is the proton energy in MeV. (A 10 keV target is $\sim 1.5 \times 10^{-4}$ grams/cm^2 .) If $G < 0.1$ the distribution will have a long tail

and an average energy significantly less than the most probable energy. If $G > 1.0$ the distribution function approaches a Gaussian.

II.B. Basic Yield Curve Characteristics

The behavior of the yield curve near threshold can be shown by assuming that the energy spread of the incident beam is zero and that the energy loss depends only on the depth of penetration. The zero degree cross section is

$$\sigma(E_p, 0) = \sigma(E_p) (1 + \gamma^2) \quad (8)$$

where γ is given by Eq. (5). For light nuclei and near threshold $\gamma^2 \gg 1$ so

$$1 + \gamma^2 \approx \gamma^2 \quad (9)$$

Consequently the total (p,n) cross section, Eq. (2), combined with Eq. (9) gives

$$\sigma(E_p, 0^\circ) \propto (E_p - E_{th})^{-1/2} \quad (10)$$

and the neutron yield becomes

$$\begin{aligned} Y(E_b, x) &\propto \int_0^x (E_b - E_{th} - (dE/dx)x)^{-1/2} dx \\ &= (E_b - E_{th})^{1/2} \quad \text{for } (E_b - E_{th}) < (dE/dx)t \\ &= (E_b - E_{th})^{1/2} - (E_b - E_{th} - (dE/dx)t)^{1/2} \\ &\quad \text{for } (E_b - E_{th}) > (dE/dx)t \end{aligned} \quad (11)$$

Obviously, in regions where the approximations are good, a plot of the square of the yield vs. E_b should extrapolate to E_{th} . The quantity we measure is magnetic field. If $(E_b - E_{th}) \ll E_{th}$, a plot of Y^2 vs. H will show a similar behavior and extrapolate to the field strength, H_{th} , which corresponds to E_{th} . A measurement

of Y vs. E_b also determines the deposit thickness since the yield reaches a maximum at $E_b - E_{th} = (dE/dx)t$. The cross section for Li-7 is given by Eq. (3) and the yield becomes

$$Y(E_b, x) \propto \ln(1 + 8.76 (E_b - E_{th})^{1/2}). \quad (12)$$

In this case a plot of the square of the yield will not be linear although it will come closer than a plot of just the yield. However, the extrapolation may be somewhat subjective.

II.C. Calculated Yield Curves

A number of yield curves were calculated using the reaction cross section energy dependence of Eq. (2) for B-11 and Eq. (3) for Li-7. The neutron detector was assumed to have a flat response and an acceptance angle of 3 deg. Symon's energy loss distribution and the beam energy resolution function given by Eq. (7) were used. Yields were obtained by a Monte Carlo evaluation of Eq. (1) to an accuracy of about 4%.

Some typical results are shown in Figs. 1 thru 4. For thick B-11 targets the Y^2 plots are linear starting about 2s above threshold and extrapolate to a point slightly below the threshold. A similar behavior was noted by Bondelid and Whiting (5) in plots of (total Yield)^{3/2}. This error is 0.1 to 0.2 keV and when very accurate thresholds are required a correction can be calculated. The Y^2 plots have a linear region only if the target is thick compared to the beam energy spread so accurate measurements should only be attempted with relatively thick targets. The Y plots may appear to be linear for a short interval but they extrapolate to a lower energy that depends on the beam energy spread. The difference is

quite small for very small beam energy spreads but increases as the spread becomes larger. Although the plots for Li-7 are not linear it is still possible to obtain fairly unambiguous intercepts for both Y and Y^2 that behave about the same as the B-11 intercepts.

II.D. Measured Yield Curves

A number of Li-7 and B-11 targets were prepared by evaporating elemental lithium and boron onto smooth tantalum target cups. Neutrons were detected by a long counter placed 1.8 meters from the target and at zero degrees with respect to the direction of the incident proton beam. Counts per unit integrated beam current were measured as a function of the magnetic field of the analyzing magnet.

A number of yield curves were measured over a period of several weeks and thresholds were determined from Y and Y^2 plots. Many of these measurements were made with 0.5 cm slit openings and at this setting the uncertainty in locating the Y^2 intercept was about 0.6 keV. The Y^2 intercept was typically ~ 1 keV higher than the Y .

Figures 5 and 6 show some results for lithium. These were selected because measurements with the buncher on or the buncher off were available for the same target with no other changes in the accelerator parameters. The Y^2 thresholds are the same in both cases while the Y threshold is lower in Fig. 6 where the energy spread is larger. This is in qualitative agreement with the calculated curves in Figs. 3 and 4.

III. NEUTRON ENERGY SPECTRA FROM LITHIUM TARGETS

Some idea of the shape of the neutron spectrum can be obtained by making measurements over a resonance where width is less than that of the spectrum. Measurements over the narrow carbon resonance near 2 MeV (see Section IV) indicated that the spectrum had a small tail. The following study was carried out to see if this was likely to have a significant effect on the energy scale.

In the very simple case of a flat (p,n) cross section, isotropic angular distribution and a proton energy loss in the target that depends only on the depth of penetration the resulting neutron energy spectrum will be a trapezoid. The width is

$$\Delta E_{\text{tot}} = \Delta E(\theta_{\text{max}}) + \Delta E(t) \quad (13)$$

where θ_{max} is the maximum angle subtended by the detector and t is the target thickness. The average energy is

$$E_{\text{av}} = E_{\text{max}} - \frac{1}{2} \Delta E_{\text{tot}}. \quad (14)$$

Including the angular distribution and energy dependence of the cross section will modify this but changes are usually small for thin targets and for $\theta_{\text{max}} < 20$ deg. Including the energy resolution of the proton beam only rounds off the corners. The condition of the lithium deposit can affect the spectrum shape. A non uniform deposit caused by a rough surface on the support plate or to excessive beam current and insufficient cooling will distort the spectrum. However, suitable experimental procedures can reduce these effects.

A factor that cannot be reduced is the tailing due to the

distribution of proton energy losses in the target as discussed in Section II.A.3. In order to investigate the size of this effect neutron energy spectra have been calculated for several target thicknesses including the angular dependence of the neutron yield, the energy spread of the incident beam and the energy loss distribution.

The results are shown in Figs. 6 through 8 and some significant quantities are listed in Table I. When G and θ_{\max} are small the spectra have significant tails. When G and θ_{\max} are larger the spectra approach the trapezoidal shape. An intermediate case shown in Fig. 7 is particularly interesting. The deposit thickness corresponds to about 17 keV and the spectra show decided tails. The size is about that suggested by transmission measurements over the 2 MeV carbon resonance. However column 6 and 7 in Table I show negligible differences in the average energy calculated from the spectra (E_5) and the average calculated from Eq. (14).

IV. THE CARBON RESONANCE

The position of the carbon resonance was obtained from a transmission measurement performed in open geometry. Neutrons were produced by the $\text{Li-7}(p,n)\text{Be-7}$ reaction as described in Section II.D. and were detected by a long counter placed at 0 deg. For most measurements the source to detector distance was 1.8 meters but for the thinnest target the distance was reduced to 1.3 meters in order to increase the count rate. A carbon disk

(3.36 g/cm²) was placed midway between the source and detector. Its 10 cm dia. made it just large enough to shadow the active face of the detector. The transmission was measured over the resonance in 1 keV steps and the peak position was obtained from an inspection of the transmission curve. The peak energy E_r , was given by

$$E_r = E_H - \frac{1}{2} \Delta E_{\text{tot}}$$

where E_H was the neutron energy corresponding to the magnetic field at the resonance peak and ΔE_{tot} was defined by Eq. (13). The accelerator was calibrated by locating the Li-7(p,n)Be-7 threshold at $1880.60 \pm .07$ keV (8) and the B-11(p,n)C-11 threshold at 3016.4 ± 1.6 keV (11). The target thickness was obtained from the difference of the lithium threshold and the peak of the zero degree yield curve (Eq.(11)).

These measurements were made at convenient times over a period of about two weeks and with several target thicknesses. The calibration was repeated before each measurement. Throughout this experiment the accelerator conditions, slit settings and calibration procedures were as similar to those used for the U-238:U-235 fission cross section ratios as was practical. The results for the different targets were consistent within the errors of the experiment and the average value of 2079.8 ± 2.9 keV agreed with the 2077 ± 2 given in BNL325 (12) and with the 2079 ± 3 found by Heaton et al. (13). When the thresholds were located by plotting the square of the yield the average value of E_r was 2078.2 ± 2.8 . These results for the individual measurements are listed in Table II. The average was 1.6 keV below that obtained by the first calibration procedure but still in very good agreement with other values.

There were several sources of error. Uncertainties in the thresholds of the calibration reactions contributed 2.3 keV at the resonance energy. The estimated error in locating the thresholds added an additional 1.8 keV. The error in locating the resonance peak was quite small for the thinnest target but was estimated to be 4 keV for the 31 keV target.

V. THE TIME-OF-FLIGHT MEASUREMENT

The magnet calibration was checked at 4.46 MeV proton energy by measuring the time-of-flight of neutrons from the $\text{Li-7}(p,n)\text{Be-7}$ reaction over a flight path with an effective length of $1149.9 \pm .9$ cm. The measurement was made at 10 deg. to the proton beam direction. The 0 deg. line would have been preferable but that passed through a steel girder about 7 meters from the source. The neutron detector was a plastic scintillator 5 cm in diameter and 0.5 cm thick. The FNG was adjusted to deliver a pulsed and bunched beam to the target with a time resolution of < 2 nanosec. The beam pulser supplied the time base. It had a frequency of 1999041 ± 4 Hz. The detector supplied the start pulse to a time-to-amplitude converter (TAC). The stop pulse came from a pickup in the beam line about 2 meters before the target. The output of the TAC was amplified and sent to a 1024 channel analyser. The gains were adjusted to give ~ 0.51 nanosec/channel.

The measurement was made by determining the change in flight path that was equivalent to one period of the beam pulser. The detector was placed on the 10 deg. line ~ 2 meters from the neutron source. The distance was measured carefully and a time

spectrum was recorded. The detector was then moved ~ 1 meter further away and the measurement repeated. This process was continued until the distance was ~ 16 meters. At ~ 8 meters the time between the stop and start signals became greater than the pulser period so the stop signal was supplied by the following beam pulse. Thus a plot of the channel number corresponding to the leading edge of the neutron pulse vs. distance gave two parallel lines. Linear fits to the data points gave

$$D_1 = 741.87 \pm 0.24 - (1.1389 \pm 0.0007)C$$

$$D_2 = 1890.08 \pm 1.02 - (1.1348 \pm .0017)C$$

where D_1 and D_2 are the distance in cm and C is the analyzer channel number. The uncertainties in the coefficients are standard deviations based on the scatter of the data. The distribution of the data was such that the minimum error in $D_2 - D_1$ occurred when $C=400$. The slopes of the two lines should be equal. However, they differ by a little over two standard deviations so the error has been doubled to give

$$D_2 - D_1 = 1149.9 \pm 0.9 \text{ cm.}$$

The corresponding energies are

$$E_n = 2.7739 \pm 0.0046 \text{ MeV}$$

$$E_p = 4.4624 \pm 0.0046 \text{ MeV.}$$

The proton energy determined from the analyzing magnet calibration was

$$E_p = 4.466 \pm 0.004 \text{ MeV.}$$

VI. CONCLUSIONS

A study of the shape of the 0 deg. yield curve for (p,n) re-

actions shows that fairly accurate thresholds can be obtained by plotting (yield)² vs. energy and extrapolating to zero. A plot of the yield vs. energy gives thresholds that may be low by as much as 2 keV. Calculation of neutron spectra show that the departure from the idealized trapezoidal shape due to the fluctuation of proton energy losses in the target deposit is large enough to affect the observed shape of narrow resonances but the effect on the energy of the resonance peak is small.

A measurement of the carbon resonance near 2 MeV produced no evidence for any systematic error in the energy scale.

The measurements reported here can be considered as either a confirmation of a calibration curve based on the lithium and boron (p,n) thresholds or as a four point calibration measurement in the proton energy range 1.88 to 4.5 MeV. The rather simple process of locating the (p,n) thresholds is sufficient to reconfirm the calibration.

REFERENCES

1. Proceedings of the NEANDC/NEACRP Specialists Meeting on Fast Neutron Fission Cross Sections of U-233, U-235, U-238 and Pu-239, June 28-30, 1976 at Argonne National Laboratory NEANDC(US)-199/L.
2. H. W. Newson, R. M. Williamson, K. W. Jones, J. W. Gibbons and H. Marshak, Phys. Rev., 108, 1294(1957).
3. W. W. Lewis, Phys. Rev., 125, 937(1962).
4. R. O. Bondelid and J. W. Butler, Phys. Rev., 130, 1078(1963).
5. R. O. Bondelid and E. E. Dowling Whiting, Phys. Rev., 134, B591(1964).
6. D. W. Palmer, W. G. Mourad, J. M. Donhowe, K. E. Nielson and R. J. Nickels, Nucl. Phys., 75, 515(1966).
7. D. W. Palmer, Nucl. Phys., 75, 529(1966).
8. J. B. Marion, Rev. Mod. Phys., 38, 660(1966).
9. K. R. Symon, Harvard University, Thesis (1948).
10. Bruno Rossi, High Energy Particles, Prentice Hall, Inc., New York, 1952.
11. E. H. Beckner, R. L. Bramblitt, G. C. Phillips and T. A. Eastwood, Phys. Rev., 123, 2100(1961).
12. S. F. Mughabghab and D. I. Garber, Neutron Cross Sections, Vol. I, Resonance Parameters, BNL 325, 3rd ed. (1973).
13. H. T. Heaton, II, J. L. Menke, R. A. Schrack and R. B. Schwartz, Nucl. Sci. Eng., 56, 27(1975).

TABLE I

mg/cm^2	ΔE_t		Δ_o (keV)	$\Delta E_n(\theta)^a$	E_s MeV	E_{av} MeV	G
	Threshold (keV)	3.5 MeV (keV)					
2×10^{-5}	2.36	1.27	0.26	11.6 0.5	1.8102 1.8160	1.8098 1.8153	.0233
1×10^{-4}	13.8	7.8	1.32	11.6 0.5	1.8077 1.8129	1.8065 1.8121	.117
2×10^{-4}	29.4	16.5	2.55	11.6 0.5	1.8028 1.8079	1.8020 1.8076	.234
4×10^{-4}	60.2	35.2	4.45	11.6 0.5	1.7934 1.7984	1.7928 1.7984	.467
1×10^{-3}	152.5	90.6	7.83	11.6 0.5	1.7651 1.7707	1.7651 1.7706	1.168

$$^a \Delta E_n(10^\circ) = 11.6 \text{ keV}$$

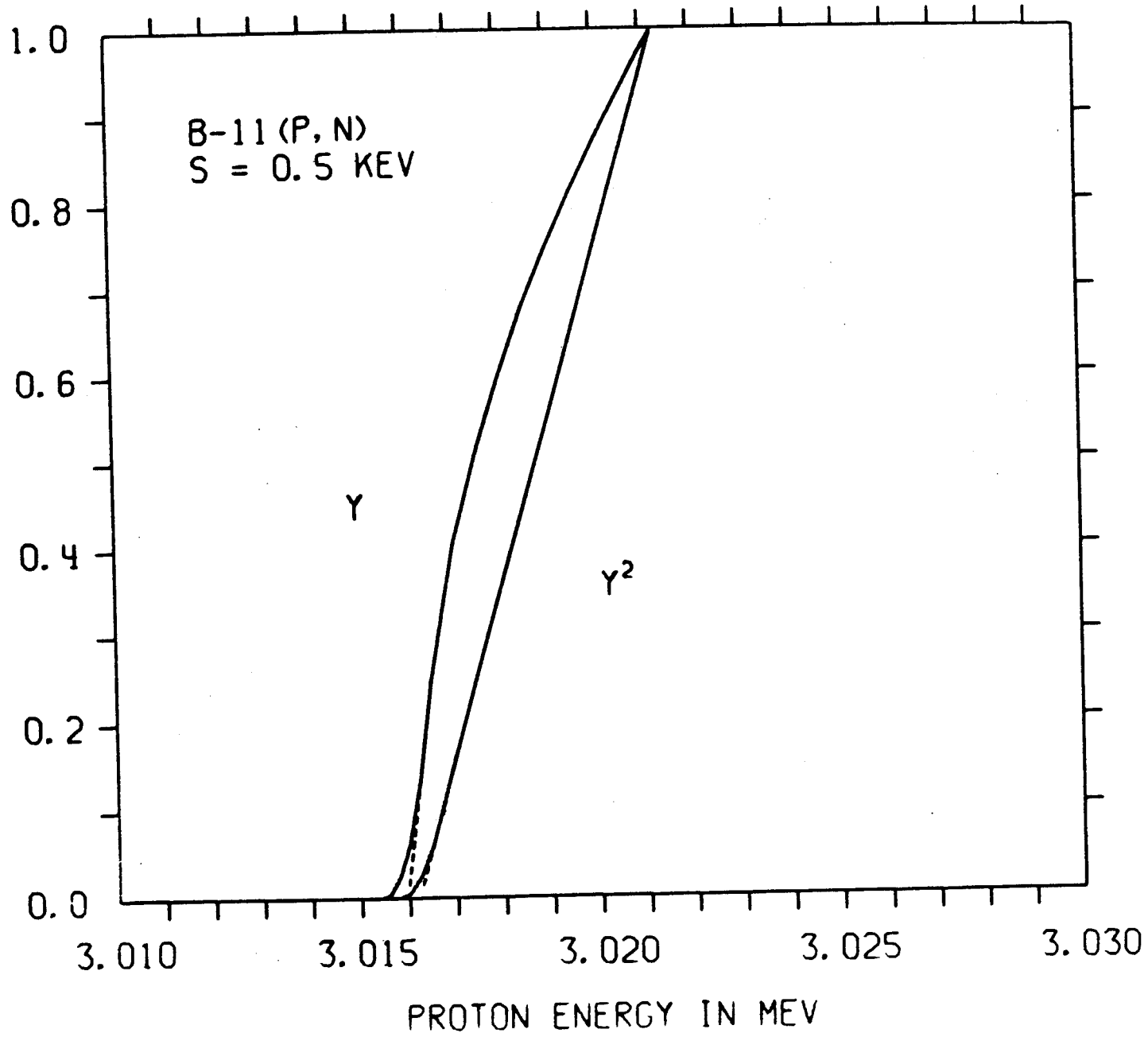
$$\Delta E_n(1^\circ) = 0.5 \text{ keV}$$

TABLE II

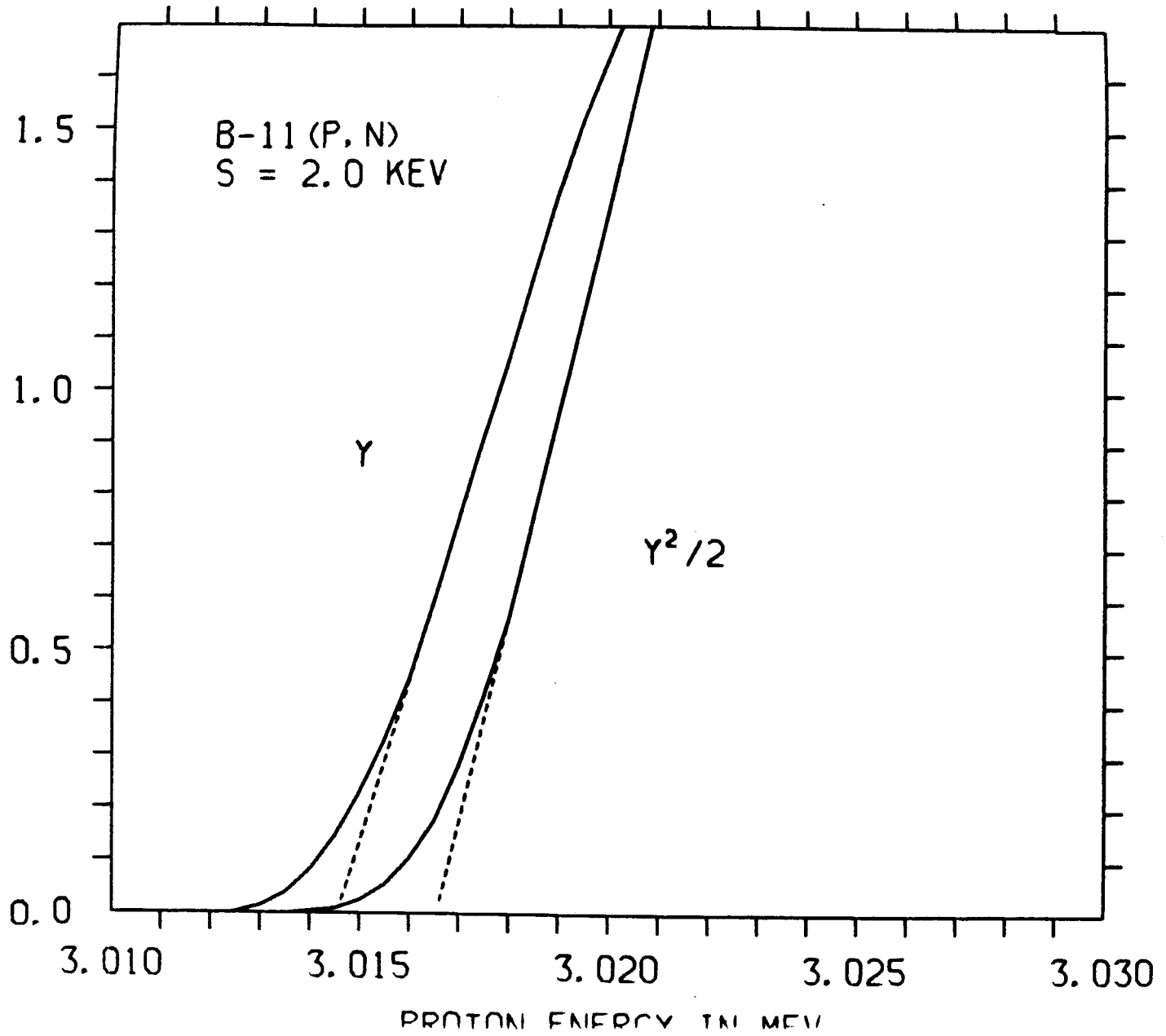
<u>Target Thickness (keV)</u>	<u>ΔE_{th} (keV)</u>	<u>E_r (keV)</u>
7.4	5.4	2079.2 \pm 3.2
7.0	5.0	2078.6 \pm 3.2
2.0	2.8	2075.6 \pm 2.7
15.2	9.9	2078.4 \pm 3.9
31.0	18.6	2079.2 \pm 4.7
	Average	2078.2 \pm 2.8

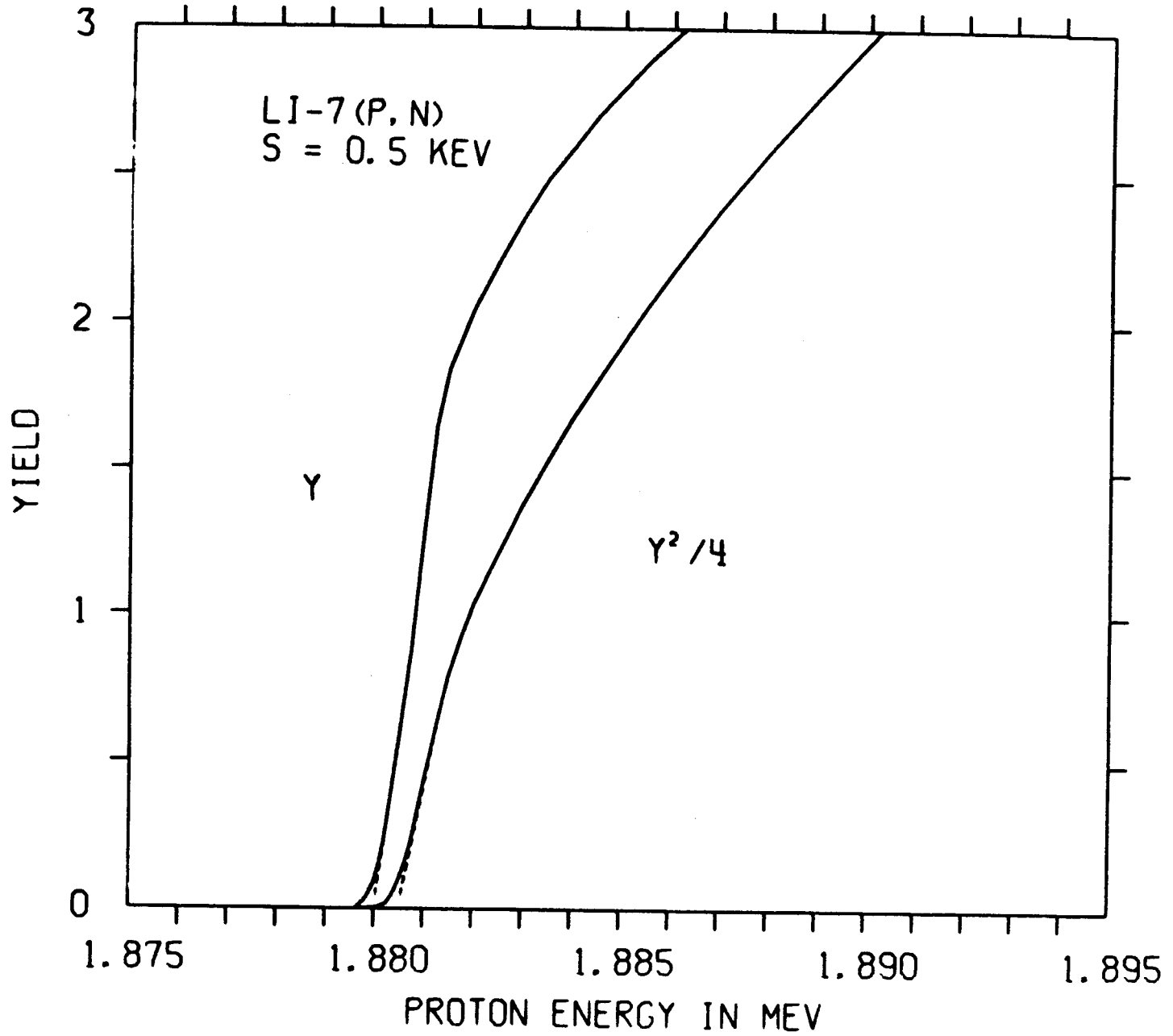
FIGURE CAPTIONS

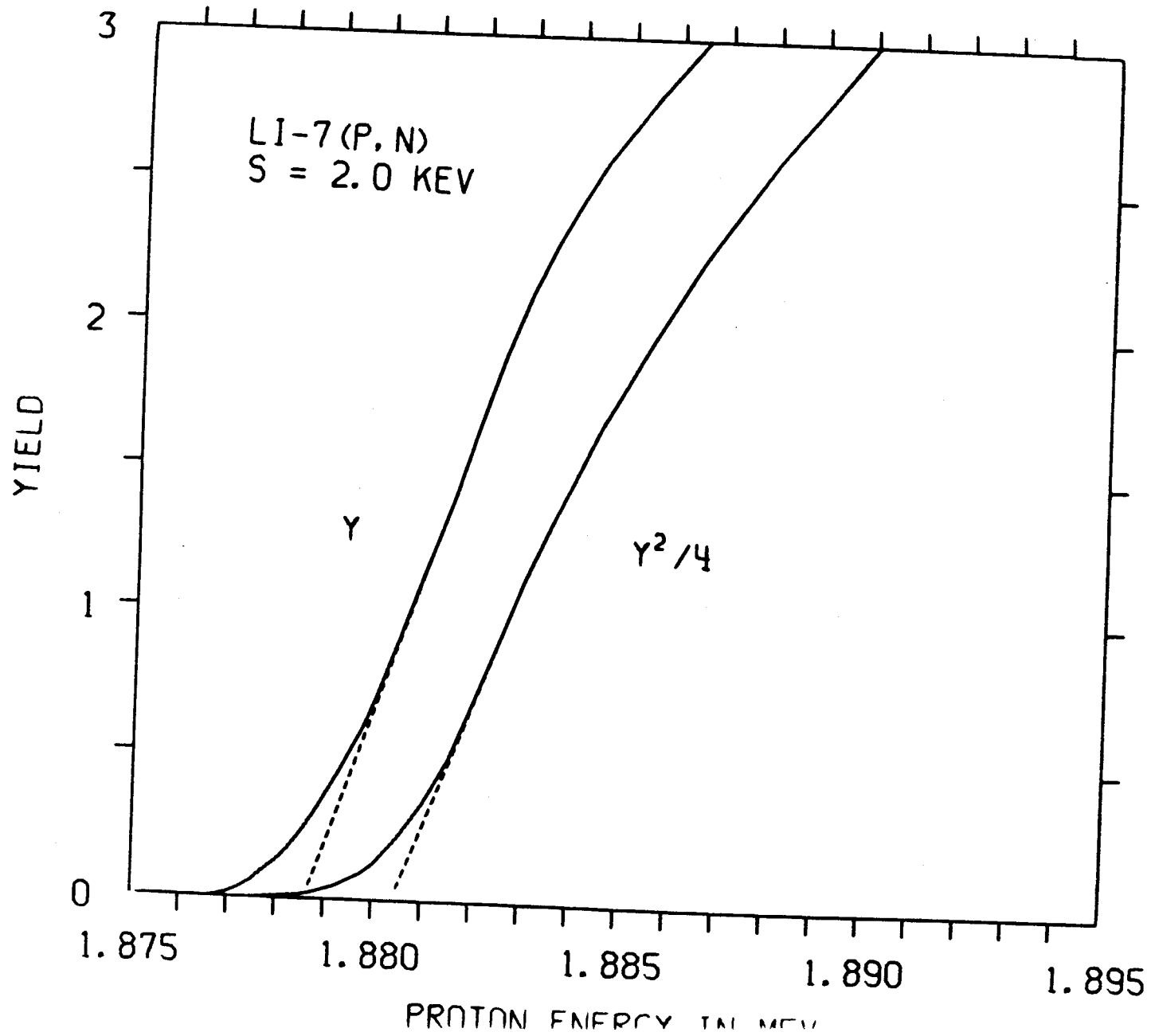
- Fig. 1. The calculated yield curve for the B-11(p,n) reaction.
 $s = 0.5$ keV
(ANL Neg. No. 116-76-394)
- Fig. 2. The calculated yield curve for the B-11(p,n) reaction.
 $s = 2.0$ keV
(ANL Neg. No. 116-76-397)
- Fig. 3. The calculated yield curve for the Li-7(p,n) reaction.
 $s = 0.5$ keV
(ANL Neg. No. 116-76-395)
- Fig. 4. The calculated yield curve for the Li-7(p,n) reaction.
 $s = 2.0$ keV
(ANL Neg. No. 116-76-396)
- Fig. 5. The measured yield curve for the Li-7(p,n) reaction with
the buncher off. $s \sim 1$ keV.
(ANL Neg. No. 116-76-401)
- Fig. 6. The measured yield curve for the Li-7(p,n) reaction with
the buncher on. $s \sim 2$ keV
(ANL Neg. No. 116-76-393)
- Fig. 7. The neutron energy spectrum for a 2.4 keV lithium target.
(ANL Neg. No. 116-76-398)
- Fig. 8. The neutron energy spectrum for a 29.4 keV lithium target.
(ANL Neg. No. 116-76-400)
- Fig. 9. The neutron energy spectrum for a 152 keV lithium target.
(ANL Neg. No. 116-76-399)



YIELD







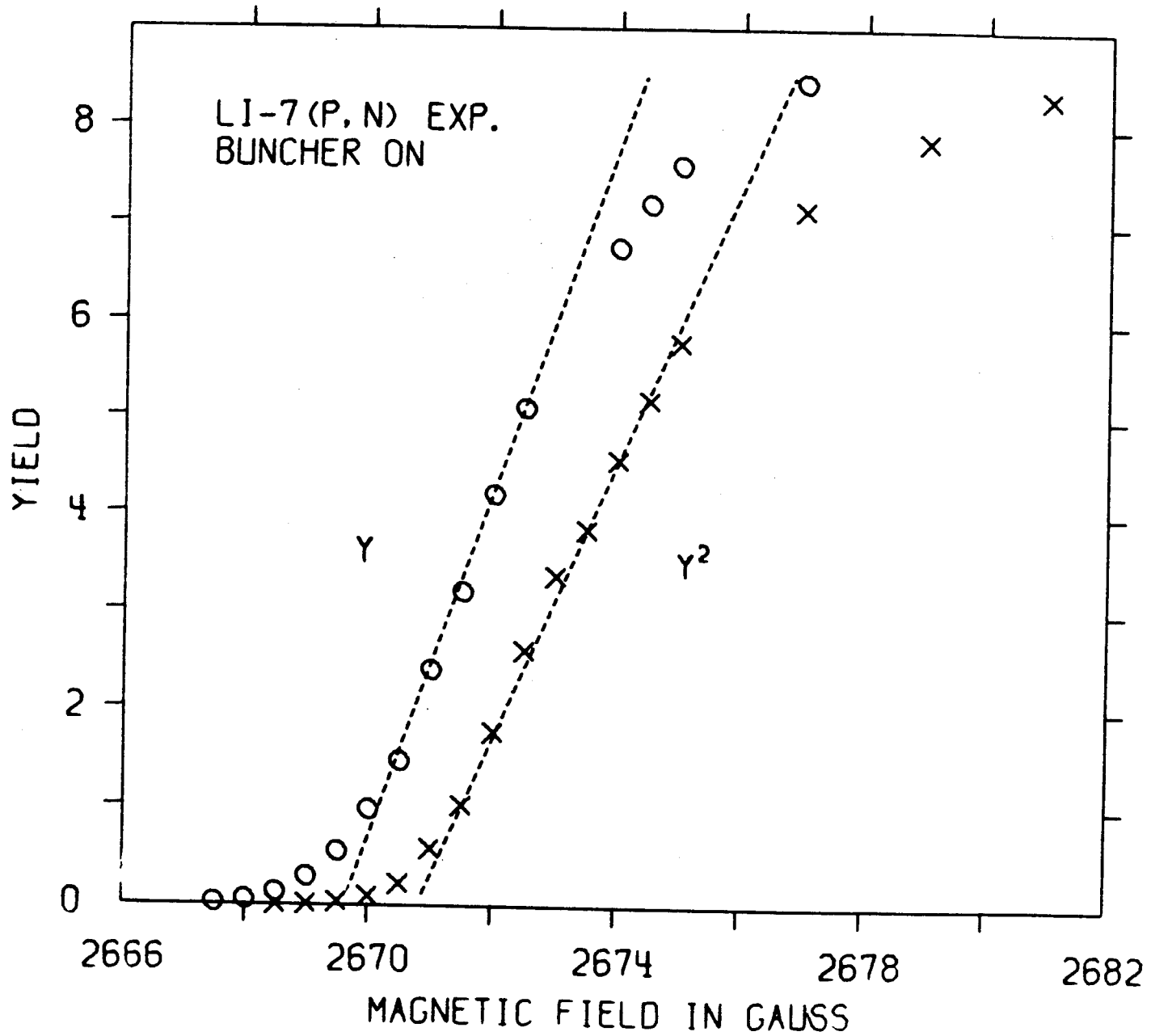


Fig. 5

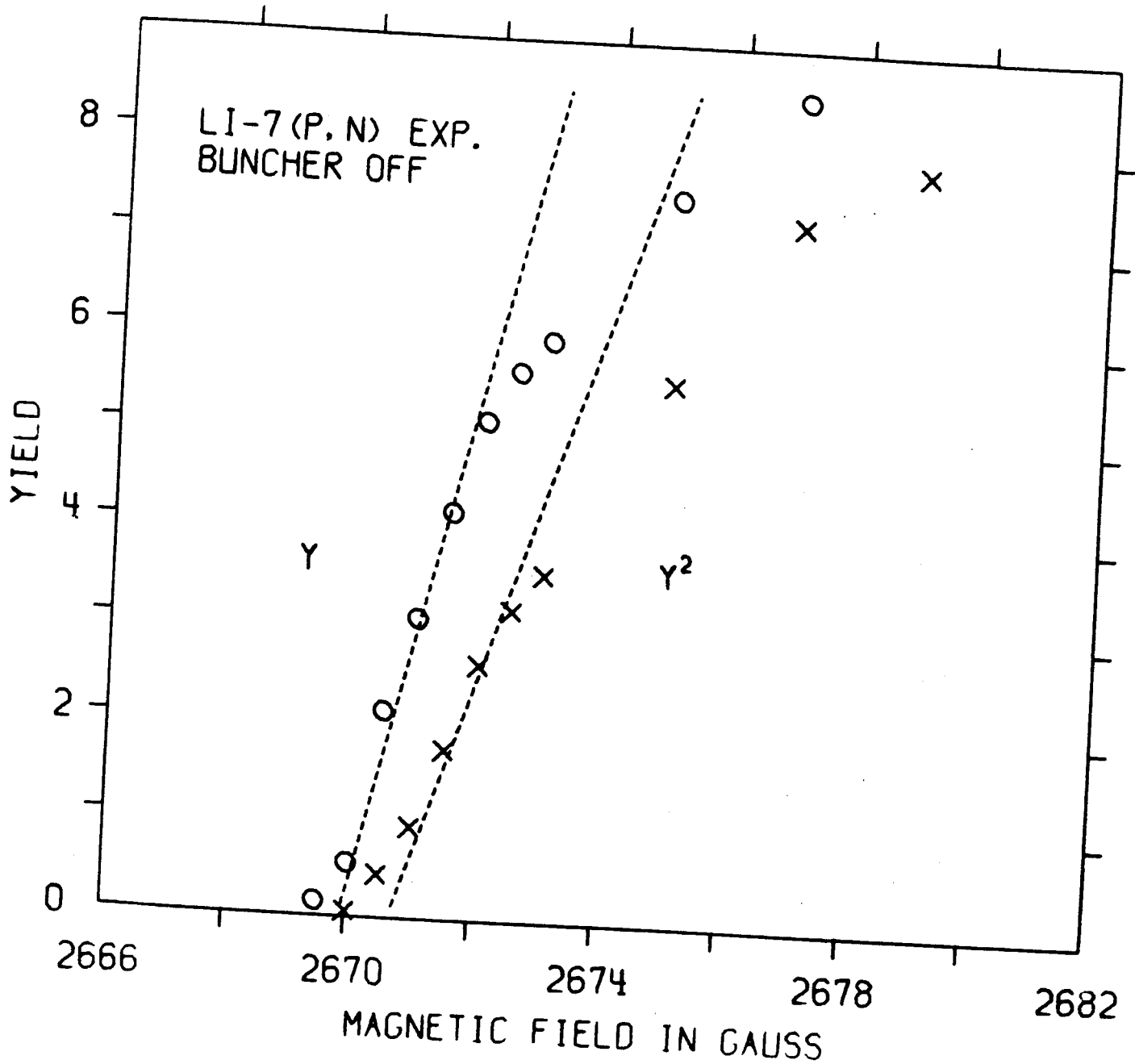


Fig. 6

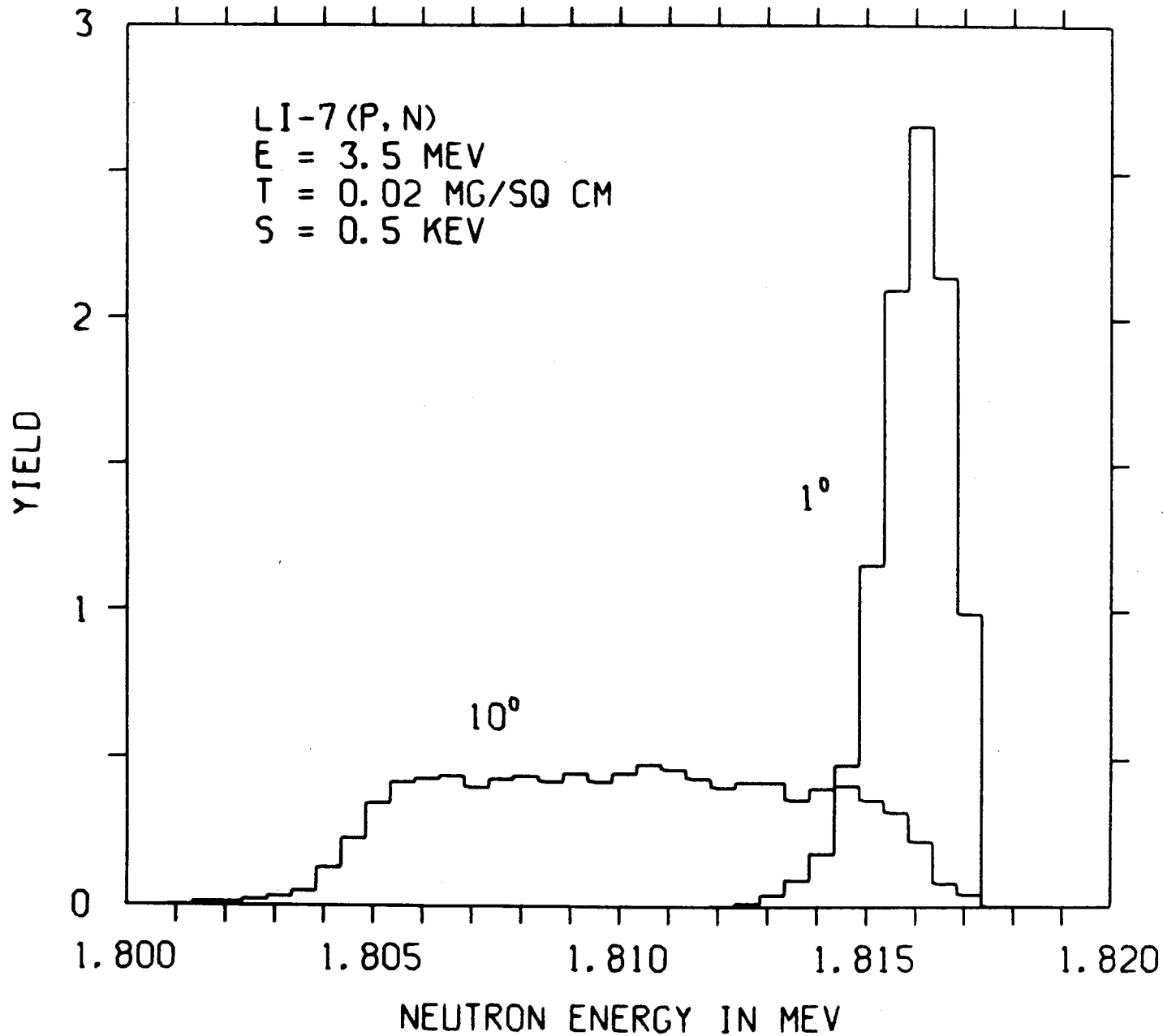
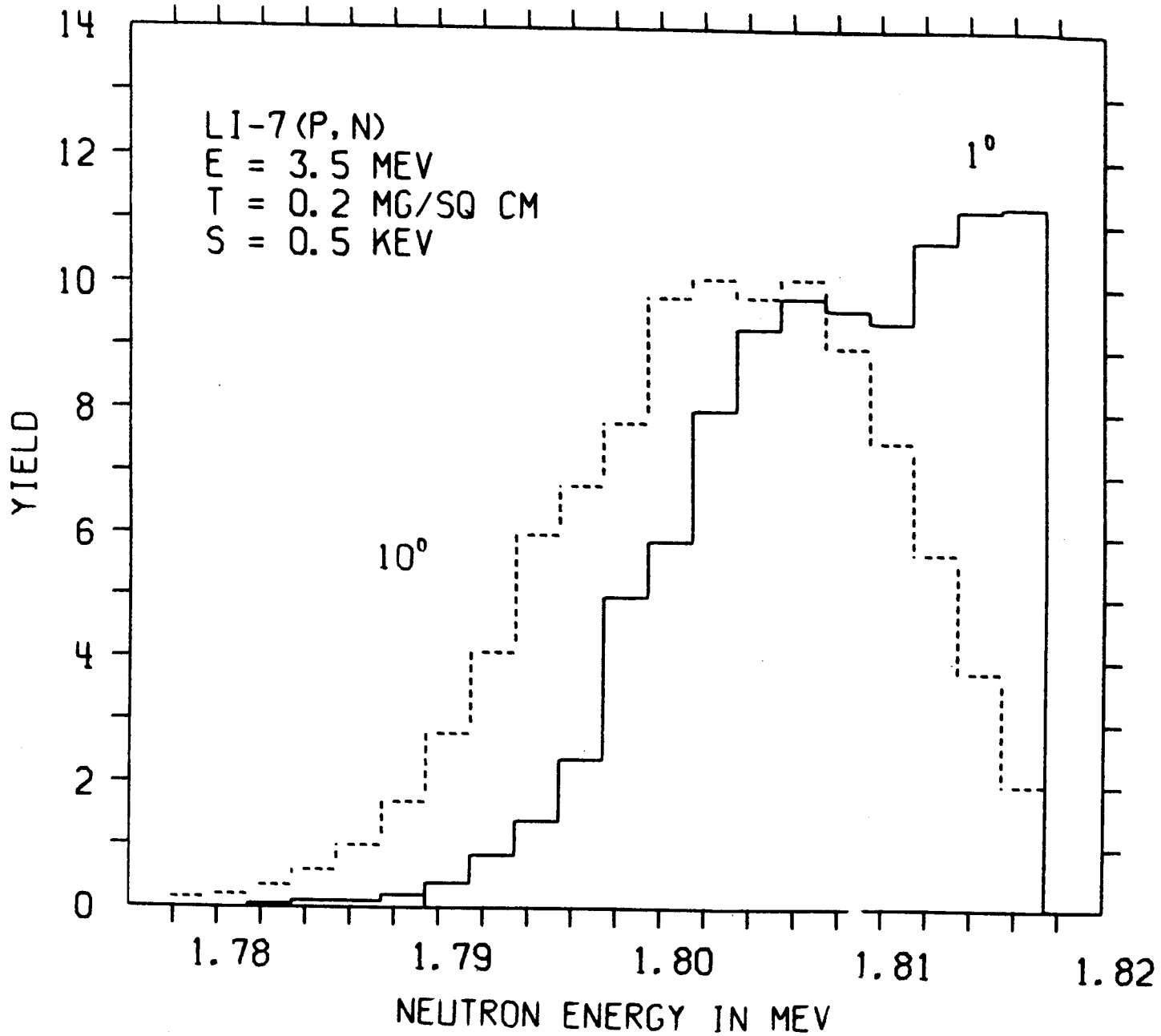


Fig. 7



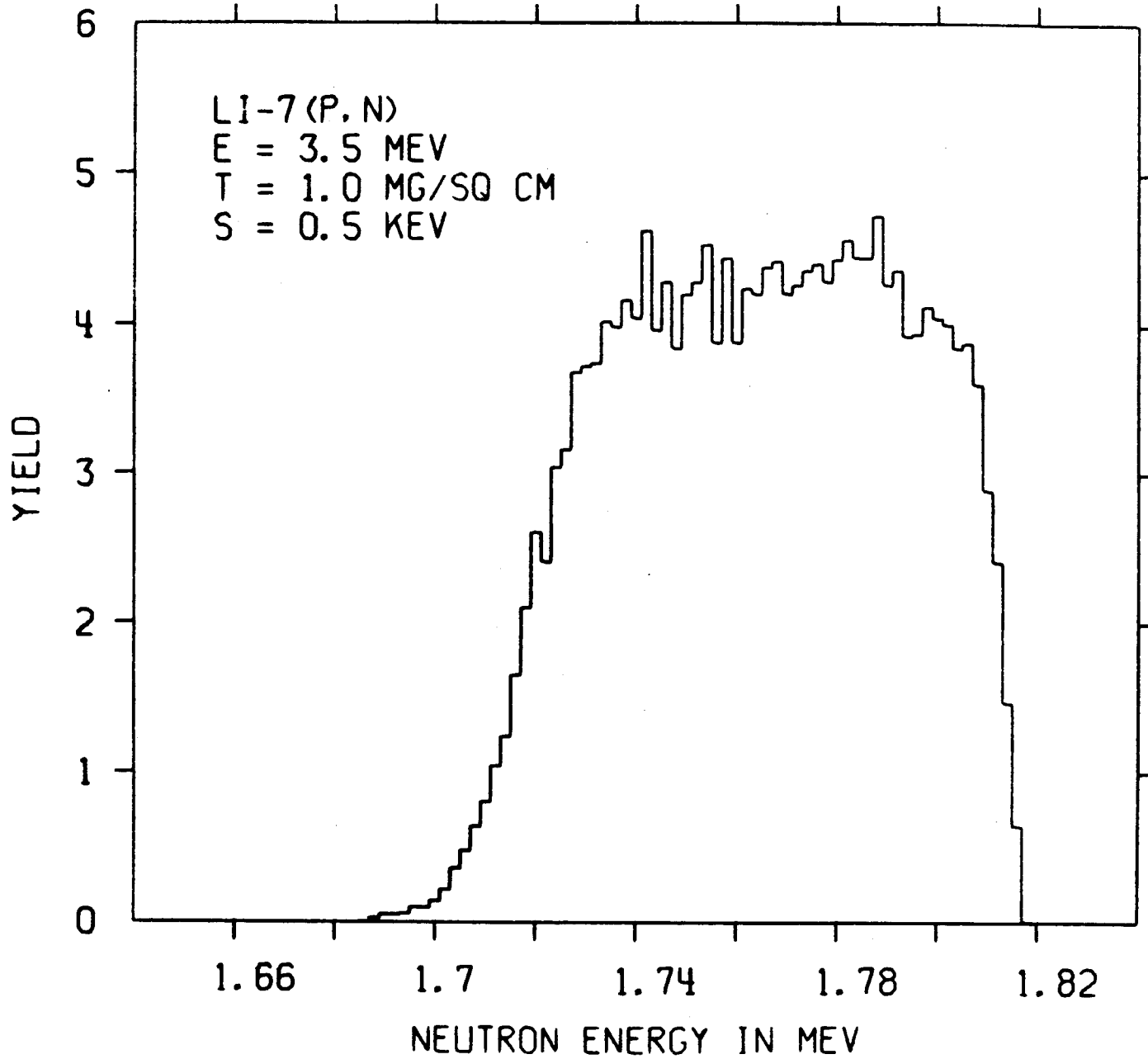


Fig. 9